

## Journal Pre-proofs

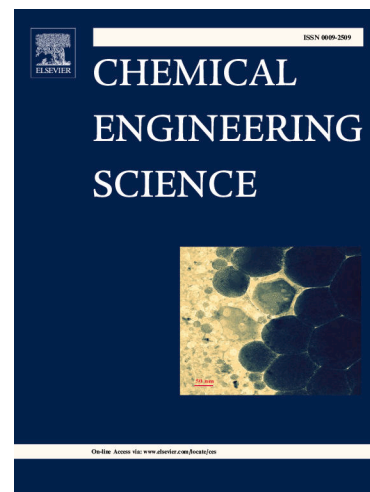
Mathematical modelling of gene delivery in patients with haemophilia B

Elnaz Jamili, Amit C. Nathwani, Vivek Dua

PII: S0009-2509(23)00629-2  
DOI: <https://doi.org/10.1016/j.ces.2023.119073>  
Reference: CES 119073

To appear in: *Chemical Engineering Science*

Received Date: 19 April 2022  
Revised Date: 13 June 2023  
Accepted Date: 5 July 2023



Please cite this article as: E. Jamili, A.C. Nathwani, V. Dua, Mathematical modelling of gene delivery in patients with haemophilia B, *Chemical Engineering Science* (2023), doi: <https://doi.org/10.1016/j.ces.2023.119073>

This is a PDF file of an article that has undergone enhancements after acceptance, such as the addition of a cover page and metadata, and formatting for readability, but it is not yet the definitive version of record. This version will undergo additional copyediting, typesetting and review before it is published in its final form, but we are providing this version to give early visibility of the article. Please note that, during the production process, errors may be discovered which could affect the content, and all legal disclaimers that apply to the journal pertain.

© 2023 Published by Elsevier Ltd.

# Mathematical Modelling of Gene Delivery in Patients with Haemophilia B

Elnaz Jamili <sup>a</sup>, Amit C. Nathwani <sup>b</sup>, and Vivek Dua <sup>a,\*</sup>

<sup>a</sup> *Department of Chemical Engineering, Centre for Process Systems Engineering, University  
College London, Torrington Place, London, WC1E 7JE, United Kingdom*

<sup>b</sup> *Department of Haematology, UCL Cancer Institute, University College London, London,  
United Kingdom*

\*Corresponding author: Vivek Dua

Phone number: +44 (0) 20 7679 0002

E-mail address: [v.dua@ucl.ac.uk](mailto:v.dua@ucl.ac.uk)

Full postal address: Department of Chemical Engineering

The Sargent Centre for Process Systems Engineering

University College London

Torrington Place

London WC1E 7JE

20 **Abstract**

21 **Type B** haemophilia is a bleeding disorder resulting from a deficiency of coagulation factor  
22 IX (FIX). Although gene therapy is a potentially curative treatment option, optimising the  
23 dosing of therapeutic genes for patients remains a challenge. Detailed simulation of gene  
24 delivery systems is required for improved understanding of the system. Hence, the purpose of  
25 this paper is to develop a modelling framework to predict the physiological response of a  
26 subject affected by type B haemophilia to a dose of vector. To address this, an integrated  
27 pharmacokinetic/pharmacodynamic (PK/PD) modelling platform was developed based on *in*  
28 *vivo* clinical data for three patients with severe haemophilia B whose functional plasma levels  
29 of FIX are less than 1% of the normal value. The plasma FIX activity was considered as the  
30 pharmacological effect while the level of serum alanine aminotransferase (ALT)  
31 demonstrated the hepatocellular toxicity. Both an individual-based modelling approach and a  
32 population modelling approach were used to estimate the physiological parameters of the  
33 developed PK/PD models. The models were then validated using data of the clinical study  
34 before being used in a simulation-based modelling approach to provide dosing  
35 recommendations. The results obtained from the study demonstrate a good prediction of the  
36 pharmacokinetics and pharmacodynamics of the vector. Model-based simulations were  
37 subsequently performed to guide initial dose selection in order to provide clinicians with  
38 better tools to make the decision-making process simpler for designing more effective  
39 treatment plans.

40

41 *Key words:* Gene delivery; Initial dose selection; Pharmacokinetic/pharmacodynamic  
42 modelling; Toxicity; Efficacy.

## 43 1 Introduction

44 Haemophilia B (HB) is a genetic bleeding disorder resulting from a deficiency or dysfunction  
45 of coagulation factor IX (FIX) caused by mutations in the gene that encodes FIX (George et  
46 al., 2017; Ramaswamy et al., 2017). Although prophylactic therapy with factor IX protein  
47 concentrates improves clinical outcomes and reduces the frequency of spontaneous bleeding,  
48 it requires frequent **intravenous** injections for the life-time of patients due to the short half-life  
49 of the protein, resulting in an inconvenient and expensive (£140,000 per year per patient)  
50 treatment (Patel et al., 2014). Thus, various strategies have been investigated for the  
51 treatment of haemophilia B including the use of bioengineered coagulation factors (Powell et  
52 al., 2013), and gene-transfer therapy (Manno et al., 2006; Nathwani et al., 2014). Gene  
53 therapy is a potentially curative treatment option as it aims to restore, modify or enhance  
54 cellular functions through the introduction of a therapeutic gene into a target cell, which is  
55 demonstrated in the work by Nathwani et al. (2001; 2006; 2007; 2011(a); 2011(b); 2014). In  
56 the clinical trial conducted by Nathwani and colleagues, a single dose of a serotype-8-  
57 pseudotyped, self-complementary (sc) adeno-associated (AAV) vector expressing a codon-  
58 optimised version of the human factor IX (hFIXco) gene was infused in patients with severe  
59 HB whose FIX activity level is <1% of normal values (Nathwani et al., 2011). hFIXco  
60 transgene was synthesised and cloned downstream of a compact synthetic liver-specific  
61 promoter (LP1) to enable packaging into scAAV vectors (scAAV2/8-LP1-hFIXco) (Patel et  
62 al., 2014). The evaluation of safety and efficacy in HB patients, having had the peripheral-  
63 vein infusion of scAAV2/8-LP1-hFIXco, was reported in the work by Nathwani et al. (2014).

64 Mathematical models are crucial tools for understanding the key mechanisms involved in  
65 biological systems, and for predicting the outcome of a given treatment plan. Mathematical  
66 modelling for gene delivery systems has evolved over the years, starting with the work by  
67 Ledley and Ledley (1994) in which the authors developed a multi-compartment **mathematical**  
68 model for studying the kinetics of cellular processes. A variety of studies have illustrated how  
69 mathematical models can be applied to gene delivery systems. Most of the works have  
70 focused on the concept of mass action kinetic model to study the critical steps involved in the  
71 process (Banks et al., 2003; Ledley & Ledley, 1994; Varga et al., 2001; 2005). A number of  
72 different computational methodologies have provided insights into the gene delivery process,  
73 including stochastic simulations (Dinh et al., 2007), quantitative structure–activity  
74 relationship (QSAR) modeling strategy (Horobin & Weissig, 2005), mechanistic spatio-  
75 temporal and stochastic model of DNA delivery (Jandt et al., 2011), semi-mechanistic model  
76 of transgene expression (Berraondo et al., 2009), and telecommunication model (Martin et  
77 al., 2015).

78 While a lot of important work has been done in the area of modelling for gene delivery  
79 systems, there are several areas which are yet to be explored adequately. We have recently  
80 developed a model-based control algorithm for both efficacy and safety to provide  
81 quantitative understanding of non-viral siRNA delivery (Jamili and Dua, 2018). Having  
82 explored the nature and purpose of quantitative analysis of *in vitro* experimental data in our  
83 previous work, this paper aims to develop a novel mathematical modelling approach, based  
84 on *in vivo* clinical data, for gene transfer of adeno-associated viral vectors in patients with  
85 haemophilia B. In this work, an integrated pharmacokinetic/pharmacodynamic model is  
86 developed using compartment modelling to describe the behaviour of scAAV2/8-LP1-  
87 hFIXco vectors in patients, which is then used in a simulation-based modelling platform for  
88 the initial dose selection with the goal of predicting the pharmacokinetics and  
89 pharmacodynamics of the vector during the therapy. A promising platform for gene delivery

90 systems is provided by using modelling techniques to determine the initial dose selection that  
 91 can be used in clinical trial simulations to determine optimal dosing recommendations.

## 92 2 Methods

### 93 2.1 Clinical Data

94 Nathwani et al. (2014) aimed to assess the efficacy and safety of factor IX gene therapy in  
 95 patients with severe HB by evaluating the stability of transgene expression and monitoring  
 96 the hepatocellular toxicity. The authors also reported the vector genomes in plasma, urine,  
 97 stool, semen and saliva, which were collected from patients at regular intervals in order to  
 98 assess vector shedding following systemic administration of scAAV2/8-LP1-hFIXco. The  
 99 clinical data is used to build an integrated PK/PD model so as to be capable of providing a  
 100 platform to guide initial dose selection.

### 101 2.2 Pharmacokinetic Modelling

102 Physiologically based pharmacokinetic (PBPK) models, while being able to offer a more  
 103 realistic picture of vector kinetics by modelling the real physiological space in the human  
 104 body, are very complex and typically require more clinical data in more compartments for the  
 105 validation of the models which is not readily available in clinical trials (Holz and Fahr, 2001).  
 106 Therefore, a mechanistically lumped PK model was developed based on the available clinical  
 107 data. **The PK model** comprised of two compartments, **plasma (P) and body fluids (BFs), to**  
 108 **illustrate the simultaneous kinetics of both plasma and metabolites** (Figure 1 and Figure 2).  
 109 **The body fluids, which encompasses data from urinary, stool, semen, and saliva,** were  
 110 lumped into **a single** compartment to represent the elimination process. This **approach was**  
 111 **adopted** because the parallel effluxes can be **merged and represented within a unified**  
 112 compartment (Holz and Fahr, 2001; Nestorov, 2003). Mathematically,

$$\frac{dC_P}{dt} = -\theta_d C_P - \theta_{el,0} C_P \quad (1)$$

$$C_P(t = 0) = C_{P0}$$

$$\frac{dC_{BF}}{dt} = \theta_{el,0} C_P - \theta_{el,1} C_{BF} \quad (2)$$

$$C_{BF}(t = 0) = C_{BF0}$$

113 where  $C_P$  (vector genome/ml) and  $C_{BF}$  (vector genome/ml) are the vector concentrations  
 114 in patient plasma and body fluids, respectively.  $\theta_d$  ( $\text{day}^{-1}$ ) represents the distribution rate  
 115 constant while  $\theta_{el,0}$  ( $\text{day}^{-1}$ ) and  $\theta_{el,1}$  ( $\text{day}^{-1}$ ) are the elimination rate constants.

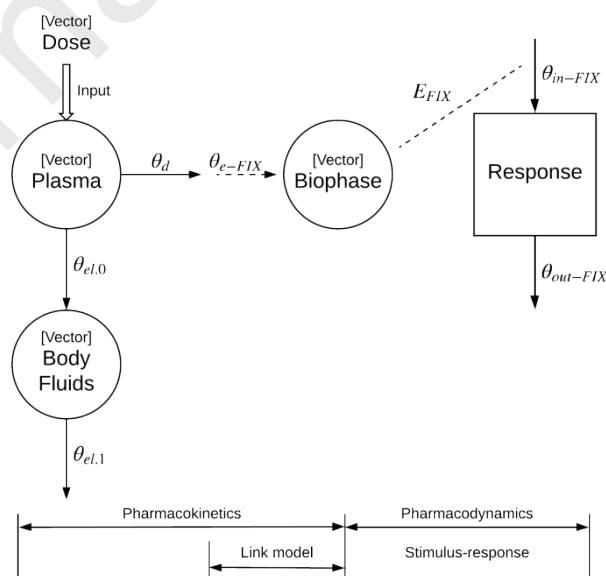
116 The developed pharmacokinetic model serves as a platform for a quantitative evaluation of  
 117 gene delivery. Equation 1 captures the rate of change of the vector concentration in patient  
 118 plasma after a single intravenous infusion of vector.

### 119 2.3 Pharmacodynamic Modelling

120 Human factor IX (hFIX) is a coagulation protein, which is synthesised in the liver, and  
 121 encoded in a gene located on the X chromosome (Howard et al., 2007; Tsang et al. 1988).  
 122 Hepatocytes, which are the most common cells type in the liver, directly secrete factor IX  
 123 into the bloodstream, where it circulates in an inactive form until needed in a response to an  
 124 injury that damages the blood vessel wall (Franchini et al., 2012). Since FIX is naturally  
 125 synthesised in the liver, the site of action for scAAV2/8-LP1-hFIXco vectors is located in the  
 126 liver compartment.

127 In order to develop a mathematical model, the plasma FIX activity has been considered as the  
 128 pharmacological effect (response), which can be treated as an objective function to be  
 129 maximised in a gene delivery optimal control problem. A physiological indirect response  
 130 model with stimulation of factors controlling the response was thought to be appropriate to  
 131 describe the vector pharmacodynamics. This is because of the time delay between the  
 132 observed pharmacological effects and vector concentration in plasma as the pharmacological  
 133 responses take time to be developed. The temporal displacement could be due to the vector  
 134 tissue distribution phenomena to reach the site of action, liver. To this purpose, a dynamic  
 135 model must be developed to link the vector concentration in the biophase or effect  
 136 compartment to a response compartment. The effect compartment model, which is also  
 137 known as the link model, can be considered as a first-order distribution model relating the  
 138 vector concentration in plasma and the biophase using a first-order constant. Once the vector  
 139 is transferred to the liver, a cascade of biological events may take place resulting in a  
 140 functional response, which can be viewed as a link model. Schematic illustration of the  
 141 integrated PK/PD model is shown in Figure 1.

142 While a more detailed representation of an integrated PK/PD approach can be developed by  
 143 incorporating the liver compartment into the PK model, the model structure, which was  
 144 developed and used in this work, had been simplified to only include the plasma and other  
 145 body fluids compartments. This is due to a lack of available data as liver biopsies are  
 146 required.



147

148 **Figure 1:** Schematic representation illustrating the relationship between kinetics and dynamics of the vector  
 149 when considering the pharmacological response (plasma FIX coagulation activity level).

150 Considering the pharmacological analysis, the rate of change of the vector concentration in  
 151 the effect (biophase) compartment,  $C_{e\_FIX}$  (vector genome/ml), can be modelled as:

$$\frac{dC_{e\_FIX}}{dt} = \theta_{e\_FIX} C_P - \theta_{in\_FIX} C_{e\_FIX} \quad (3)$$

152 where  $C_P$  (vector genome/ml) is the concentration of vector in the plasma compartment of  
 153 the pharmacokinetic model, linked to the effect compartment, with the first-order rate  
 154 constant  $\theta_{e\_FIX}$  ( $\text{day}^{-1}$ ).

155 The plasma FIX coagulation activity level,  $R_{FIX}$  (% of the normal value - IU/deciliter),  
 156 which is of interest in our case, is formulated as a function of the concentration in the effect  
 157 compartment with the use of an effect-concentration model. The differential equation for the  
 158 observed pharmacological effect, factor IX activity level, can be expressed as:

$$\frac{dR_{FIX}}{dt} = \theta_{in\_FIX} E_{FIX} - \theta_{out\_FIX} R_{FIX} \quad (4)$$

159 where the *rate in* and *rate out* of the response compartment are governed by  $\theta_{in\_FIX}$  ( $\text{day}^{-1}$ )  
 160 and  $\theta_{out\_FIX}$  ( $\text{day}^{-1}$ ).

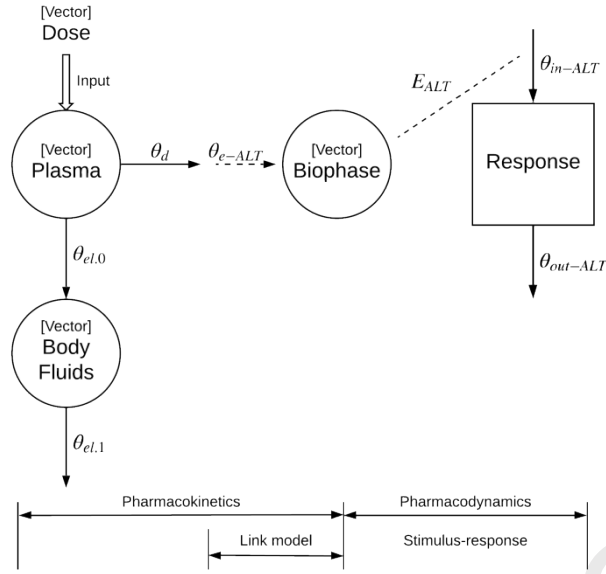
161 Note that the effect compartment model should be selected with an appropriate effect  
 162 equation. In this study, the response is modelled by means of a linear transduction function in  
 163 which the vector concentration is proportionally related to a pharmacological response  
 164 (Gabrielsson and Weiner, 2010). Therefore,

$$E_{FIX} = k C_{e\_FIX} \quad (5)$$

165 where  $k$  is the slope parameter, which is assumed to be  $k = 1$  in order to **simplify the model**  
 166 **to** help to mitigate the numerical difficulties.

## 167 2.4 Incorporating the Toxicological Model

168 The PD model may be extended to incorporate the toxicological responses that captures the  
 169 liver toxicity, which was observed in the clinical study by Nathwani and colleagues as the  
 170 primary endpoint of their study was the safety evaluation of the vector infusion at different  
 171 doses. The reported level of serum alanine aminotransferase (ALT) over time demonstrates  
 172 the hepatocellular toxicity. ALT is an enzyme which is found in serum and organ tissues such  
 173 as liver. The ALT level is the most widely used clinical biomarker of liver function, which  
 174 may be elevated as a result of the leakage from the damaged hepatocytes into the plasma  
 175 following hepatocellular injury (Washington and Van Hoosier, 2012).



176

177 **Figure 2:** Schematic representation illustrating the relationship between kinetics and dynamics of the vector  
 178 when considering the toxicological response (ALT level).

179 In this section, the structure of the PD model has been kept the same as in Section 2.3.  
 180 Assuming an indirect response model with stimulation of factors controlling the toxicological  
 181 response (Figure 2), the rate of change of the vector concentration in the effect (biophase)  
 182 compartment,  $C_{e\_ALT}$  (vector genome/ml), can be modelled as:

$$\frac{dC_{e\_ALT}}{dt} = \theta_{e\_ALT} C_P - \theta_{in\_ALT} C_{e\_ALT} \quad (6)$$

183 where  $C_P$  (vector genome/ml) is the concentration of vector in the plasma compartment of  
 184 the pharmacokinetic model, linked to the effect compartment, with the first-order rate  
 185 constant  $\theta_{e\_ALT}$  ( $\text{day}^{-1}$ ).

186 The ALT level,  $R_{ALT}$  (IU/liter), is formulated as a function of the concentration in the effect  
 187 compartment with the use of an effect-concentration model:

$$\frac{dR_{ALT}}{dt} = \theta_{in\_ALT} E_{ALT} - \theta_{out\_ALT} R_{ALT} \quad (7)$$

$$E_{ALT} = k C_{e\_ALT} \quad (8)$$

188 where the *rate in* and *rate out* of the response compartment are governed by  $\theta_{in\_ALT}$  ( $\text{day}^{-1}$ )  
 189 and  $\theta_{out\_ALT}$  ( $\text{day}^{-1}$ ), and  $k = 1$ .



### 190 3 Results and Discussion

191 The proposed modelling framework will be evaluated for three patients with severe HB who  
 192 had received intermediate dose of vector,  $6 \times 10^{11}$  vector genomes (vg) per kilogram (kg) of  
 193 body weight, (patient 4); and high dose of vector,  $2 \times 10^{12}$  vg per kg, (patients 6 and 9). **The**  
 194 **mean weight was 80.7 kg.** Table 1 summarises the key characteristics of the patients.

195 **Table 1:** Key characteristics of the patients at baseline, according to vector dose. Adapted from Nathwani et al.  
 196 (2014).

Characteristic	Vector Dose, $6 \times 10^{11}$ vg/kg	Vector Dose, $2 \times 10^{12}$ vg/kg	
	Patient 4	Patient 6	Patient 9
<b>Sex</b>	Male	Male	Male
<b>Age (yr)</b>	29	27	44
<b>Factor IX prophylaxis</b>	Once weekly	Three times weekly	On demand
<b>HIV status</b>	Negative	Negative	Negative
<b>Hepatitis C status</b>	Negative	Negative	Positive

197 The results obtained from this study will be presented in two parts. First, the results of the  
 198 parameter estimation problem will be discussed in Section 3.1. Then, a number of dynamic  
 199 simulations will be presented in Section 0 for initial dose selection.  
 200

#### 201 3.1 Parameter Estimation

202 Having the clinical data and the PK/PD model, given by Equations 1–8, the parameter  
 203 estimation problem was formulated as an optimisation problem, and solved using the  
 204 analytical solutions of the PK and PD models, which were obtained by using Mathematica.  
 205 Since the spread of values in the PK clinical data set is large, the PK parameter estimation  
 206 problem was performed using both absolute and scaled objective functions. The full set of  
 207 model parameters and state variables are listed in Table 2.

208 **Table 2:** Model parameters and state variables of the PK/PD model.

Symbol	Description	Units
--------	-------------	-------

$\Psi_k$	The vector of the state variables in compartment $k$	
$C_P$	Vector concentration in the plasma compartment	vg/ml
$C_{BF}$	Vector concentration in the body fluids compartment	vg/ml
$C_{e\_FIX}$	Vector concentration in the biophase (effect) compartment when considering the pharmacological response (FIX coagulation activity level)	vg/ml
$C_{e\_ALT}$	Vector concentration in the biophase (effect) compartment when considering the toxicological response (ALT level)	vg/ml
$R_{FIX}$	Plasma factor IX coagulation activity level	IU/dl
$R_{ALT}$	ALT level	IU/L
$\theta$	The vector of the model parameters	
$\theta_d$	Distribution rate constant	day <sup>-1</sup>
$\theta_{el,0}$	Elimination rate constant	day <sup>-1</sup>
$\theta_{el,1}$	Elimination rate constant	day <sup>-1</sup>
$\theta_{e\_FIX}$	Rate constant linking a kinetic model and a dynamic model when considering the pharmacological response (FIX coagulation activity level)	day <sup>-1</sup>
$\theta_{e\_ALT}$	Rate constant linking a kinetic model and a dynamic model when considering the toxicological response (ALT level)	day <sup>-1</sup>
$\theta_{in\_FIX}$	The <i>rate in</i> of the pharmacological response compartment ( $R_{FIX}$ )	day <sup>-1</sup>
$\theta_{out\_FIX}$	The <i>rate out</i> of the pharmacological response compartment ( $R_{FIX}$ )	day <sup>-1</sup>
$\theta_{in\_ALT}$	The <i>rate in</i> of the toxicological response compartment ( $R_{ALT}$ )	day <sup>-1</sup>
$\theta_{out\_ALT}$	The <i>rate out</i> of the toxicological response compartment ( $R_{ALT}$ )	day <sup>-1</sup>

**Err<sub>absolute</sub>** Absolute objective function

**Err<sub>scaled</sub>** Scaled objective function

**$\hat{\Psi}_k$**  The vector of the observed clinical data in compartment  $k$

209

210 The generic mathematical formulation of the parameter estimation problem is as follows:

$$\text{Err}_{\text{absolute}} = \min_{\theta, \Psi(t)} \sum_{p \in P} \sum_{k \in K} \{\Psi_k(t_p) - \hat{\Psi}_k(t_p)\}^2 \quad (9)$$

211 or

$$\text{Err}_{\text{scaled}} = \min_{\theta, \Psi(t)} \sum_{p \in P} \sum_{k \in K} \left\{ \frac{\Psi_k(t_p) - \hat{\Psi}_k(t_p)}{\hat{\Psi}_k(t_p)} \right\}^2 \quad (10)$$

212 subject to the analytical solutions of the PK/PD model. **For more details, please see Equations**  
 213 **1-6 in the Supplementary Appendix.**

214 To carry out parameter estimation for the system, first, PK/PD parameters were estimated  
 215 individually for each patient, which could be useful for the development of personalised gene  
 216 therapy. Then, PK and PD parameters were estimated for all patients simultaneously, which  
 217 were used for the initial dose selection, aiming at predicting the physiological response of a  
 218 patient to a dose of vector. For individually estimated PK/PD parameters, the analysis was  
 219 dependent on the initial vector concentration, whereas the simultaneous parameter estimation  
 220 was dose-dependent. Table 3 and Table 4 summarise the parameter estimation results for  
 221 individually and simultaneously estimated parameters. The estimated parameter values were  
 222 then used for dynamic simulations using Orthogonal Collocation on Finite Elements (OCFE),  
 223 which were carried out for the validation of the model, with a view to pave the way for  
 224 control of gene delivery in future work. Note that the model parameters are specific to a  
 225 patient and may vary between patients (inter-patient) and also within individual patients  
 226 (intra-patient). There are different factors that affect inter- and intra-patient variability, such  
 227 as age, **sex**, body weight, health condition and activity levels.

228 **Table 3:** Estimated PK/PD model parameters, individually for each patient.

Patient 4 (P.4)				
		Estimated parameters (day <sup>-1</sup> )		
<b>PK Model</b>	Absolute OBJ <sup>▲</sup>	$\theta_d = 1.5710559$	$\theta_{el,0} = 1.0506840$	$\theta_{el,1} = 2.1366106$

	Scaled OBJ*	$\theta_d = 2.5971076$	$\theta_{el,0} = 0.0247028$	$\theta_{el,1} = 0.4823376$
<b>PD Model</b>	FIX	$\theta_{e\_FIX} = 9.7701316$	$\theta_{in\_FIX} = 0.0016288$	$\theta_{out\_FIX} = 0.0631596$
	ALT	$\theta_{e\_ALT} = 18.4752261$	$\theta_{in\_ALT} = 0.0005428$	$\theta_{out\_ALT} = 0.0074621$

229

<b>Patient 6 (P.6)</b>				
		Estimated parameters (day <sup>-1</sup> )		
<b>PK Model</b>	Absolute OBJ*	$\theta_d = 2.1140705$	$\theta_{el,0} = 0.0073093$	$\theta_{el,1} = 0.5635716$
	Scaled OBJ*	$\theta_d = 2.0194024$	$\theta_{el,0} = 0.0910754$	$\theta_{el,1} = 1.7344535$
<b>PD Model</b>	FIX	$\theta_{e\_FIX} = 21.1668725$	$\theta_{in\_FIX} = 0.0003748$	$\theta_{out\_FIX} = 0.0158966$
	ALT	$\theta_{e\_ALT} = 0.3656878$	$\theta_{in\_ALT} = 0.0028681$	$\theta_{out\_ALT} = 0.0005408$

230

<b>Patient 9 (P.9)</b>				
		Estimated parameters (day <sup>-1</sup> )		
<b>PK Model</b>	Absolute OBJ*	$\theta_d = 0.1593991$	$\theta_{el,0} = 1.1246204$	$\theta_{el,1} = 0.6580731$
	Scaled OBJ*	$\theta_d = 0.9911402$	$\theta_{el,0} = 0.3439847$	$\theta_{el,1} = 0.4674078$
<b>PD Model</b>	FIX	$\theta_{e\_FIX} = 2.0086934$	$\theta_{in\_FIX} = 0.0012088$	$\theta_{out\_FIX} = 0.0038267$
	ALT	$\theta_{e\_ALT} = 6.4510203$	$\theta_{in\_ALT} = 0.0010856$	$\theta_{out\_ALT} = 0.0033077$

231

232 **Table 4:** Estimated PK/PD model parameters, for all patients simultaneously.

Patients 4, 6, and 9 (P.4-6-9)				
		Estimated parameters (day <sup>-1</sup> )		
<b>PK Model</b>	Absolute OBJ <sup>♠</sup>	$\theta_d = 1.5511141$	$\theta_{el,0} = 0.4723049$	$\theta_{el,1} = 0.7640243$
	Scaled OBJ <sup>♣</sup>	$\theta_d = 7.1957447$	$\theta_{el,0} = 2.0910047$	$\theta_{el,1} = 1.7113180$
<b>PD Model</b>	FIX	$\theta_{e\_FIX} = 11.2140501$	$\theta_{in\_FIX} = 0.0005731$	$\theta_{out\_FIX} = 0.0737731$
	ALT	$\theta_{e\_ALT} = 0.6582939$	$\theta_{in\_ALT} = 0.0007284$	$\theta_{out\_ALT} = 0.0014742$

233

234 ♠ – Solved the parameter estimation problem using an absolute objective function (Equation 9).

235 ♣ – Solved the parameter estimation problem using a scaled objective function (Equation 10).

236

237 In order to visualise the variance between the estimated PK/PD parameters across different  
 238 patients, the results are also graphically shown in Figure 3. Note that in the following figure,  
 239 P.4, P.6, and P.9 refer to Patient 4, Patient 6, and Patient 9 respectively, where the PK and PD  
 240 parameters were estimated individually for each patient. However, P.4-6-9 refers to the  
 241 population modelling approach in which each PK and PD parameters were estimated for all  
 242 patients simultaneously.

243

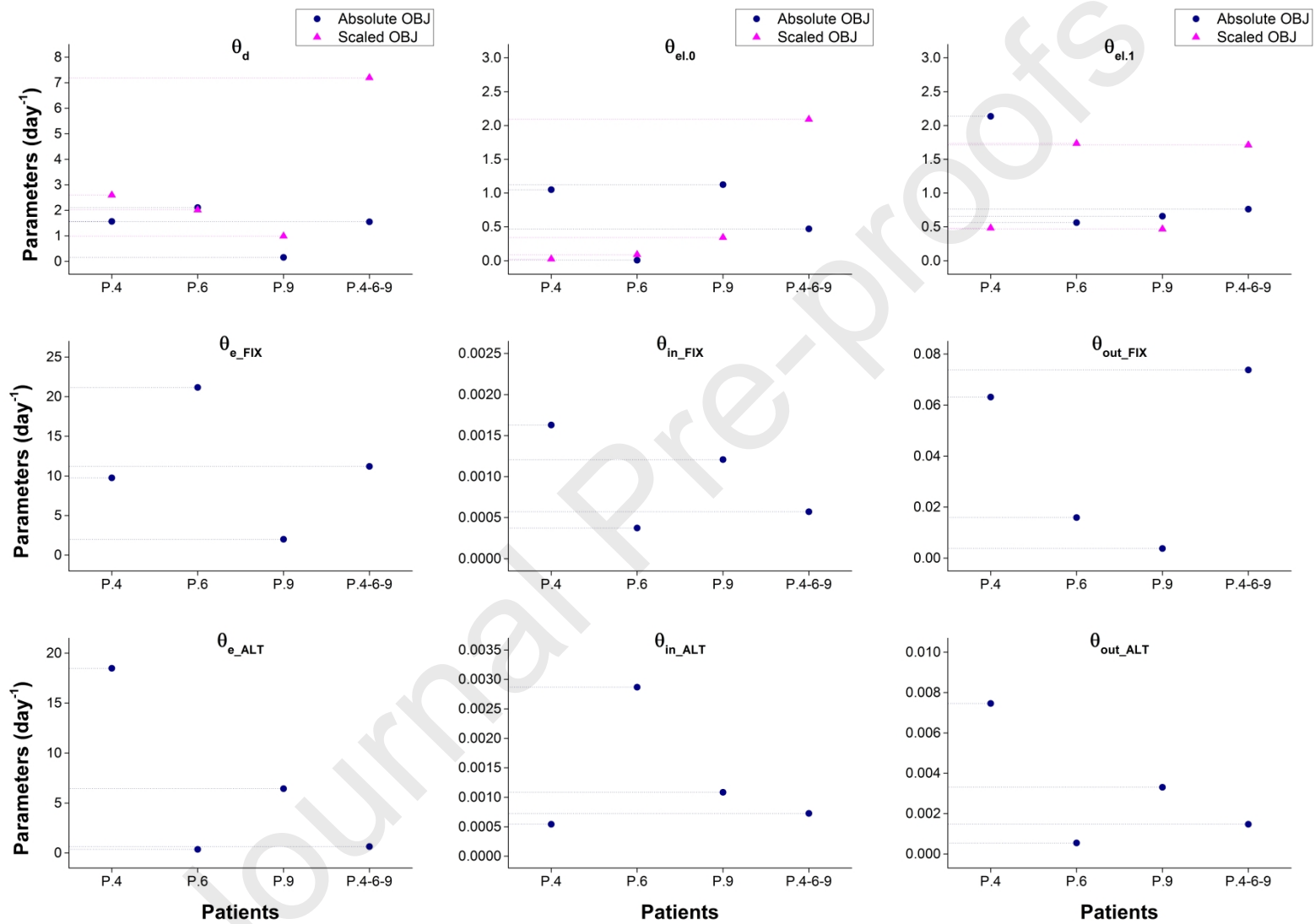


Figure 3: Estimated PK/PD parameters across different patients.

244

245

246 In Figure 3, the variability of the estimated model parameters across different patients could  
247 be associated with the inter-patient variability, suggesting that the personalised gene therapy  
248 using an individual modelling approach would make more sense because the  
249 pharmacokinetics and pharmacodynamics of the vector can vary between patients. However,  
250 to gain more insights into the process, both the individual modelling approach (solving the  
251 parameter estimation problem for each patient individually) and the population modelling  
252 approach (solving the parameter estimation problem for all patients simultaneously) were  
253 considered in the present work.

254 It is important to note here that the estimated model parameters could vary for different initial  
255 guesses used for the parameter estimation problem. Difficulties arise from both the existence  
256 of local minima and non-identifiability (Degaspero et al., 2017). The solver may find different  
257 local minima when started from different starting points due to the non-convexity of the  
258 objective function. Global optimisation-based algorithms were applied; however, the model  
259 was unable to converge to find a global optimal solution. Furthermore, the identifiability  
260 issue is concerned with the theoretical existence of unique solutions to the parameter  
261 estimation problem. Hence, there are various sets of parameter values that fit the clinical data  
262 equally well. Different strategies, such as model reformulation, model reduction, or  
263 generating additional clinical data can be used to overcome the identifiability problem  
264 (Degaspero et al., 2017). Sensitivity analysis was performed to investigate the sensitivities of  
265 state variables relative to small changes in model parameters at the steady state (Table 5 and  
266 Table 6). All relative sensitivities of model variables to changes in parameters are smaller  
267 than 1 in absolute value, meaning that perturbations in value of the parameters are attenuated.

268 **Table 5:** Model sensitivity matrix for the individual modelling approach.

Parameters	Individual Modelling Approach											
	Patient 4				Patient 6				Patient 9			
	$C_P$	$C_{BF}$	$R_{FIX}$	$R_{ALT}$	$C_P$	$C_{BF}$	$R_{FIX}$	$R_{ALT}$	$C_P$	$C_{BF}$	$R_{FIX}$	$R_{ALT}$
$\theta_{d\_absolute}$	- 0.000001	- 0.000001	-	-	- 0.000002	- 0.000001	- 0.2	- 0.14	- 0.000001	- 0.000001	- 0.03	- 0.08
$\theta_{el.0\_absolute}$	- 0.000001	- 0.000001	-	-	- 0.000001	0.000001	- 0.01	- 0.01	- 0.000002	- 0.000001	- 0.18	- 0.57
$\theta_{el.1\_absolute}$	-	- 0.000002	-	-	-	- 0.000003	-	-	-	- 0.000002	-	-
$\theta_{d\_scaled}$	- 0.000002	- 0.000003	- 0.04	- 0.6	- 0.000002	- 0.000001	-	-	- 0.000002	- 0.000001	-	-
$\theta_{el.0\_scaled}$	- 0.000001	0.000002	- 0.01	- 0.01	- 0.000001	0.000001	-	-	- 0.000001	0.000001	-	-
$\theta_{el.1\_scaled}$	-	- 0.000025	-	-	-	- 0.000002	-	-	-	- 0.000002	-	-
$\theta_{e\_FIX}$	-	-	0.03	-	-	-	0.18	-	-	-	0.18	-
$\theta_{in\_FIX}$	-	-	- 0.03	-	-	-	0.11	-	-	-	0.17	-



$\theta_{out\_FIX}$	-	-	- 0.04	-	-	-	- 0.21	-	-	-	- 0.27	-
$\theta_{e\_ALT}$	-	-	-	0.57	-	-	-	0.12	-	-	-	0.62
$\theta_{in\_ALT}$	-	-	-	0.3	-	-	-	- 0.02	-	-	-	0.48
$\theta_{out\_ALT}$	-	-	-	- 0.68	-	-	-	- 0.44	-	-	-	- 0.81

269  
270

**Table 6:** Model sensitivity matrix for the population modelling approach.

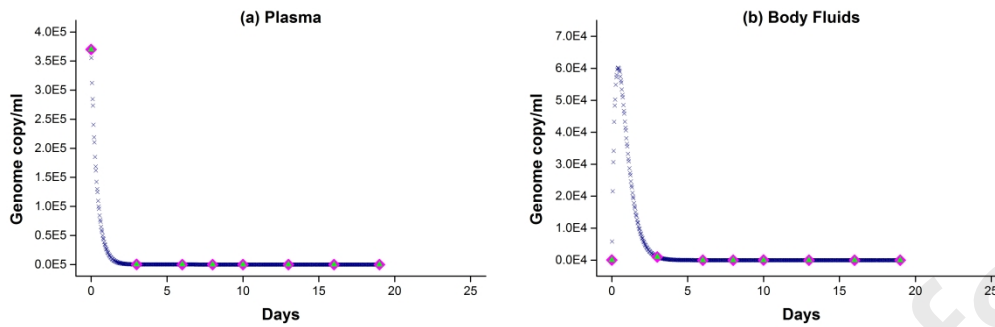
Parameters	Population Modelling Approach											
	Patient 4				Patient 6				Patient 9			
	$C_P$	$C_{BF}$	$R_{FIX}$	$R_{ALT}$	$C_P$	$C_{BF}$	$R_{FIX}$	$R_{ALT}$	$C_P$	$C_{BF}$	$R_{FIX}$	$R_{ALT}$
$\theta_{d\_absolute}$	- 0.000002	- 0.000001	- 0.03	- 0.1	- 0.000002	- 0.000001	- 0.15	- 0.53	- 0.000002	- 0.000001	- 0.22	- 0.49
$\theta_{el0\_absolute}$	- 0.000001	0.000001	- 0.01	- 0.03	- 0.000001	0.000001	- 0.05	- 0.16	- 0.000001	0.000001	- 0.07	- 0.15
$\theta_{el1\_absolute}$	-	- 0.000002	-	-	-	- 0.000004	-	-	-	- 0.000002	-	-
$\theta_{d\_scaled}$	- 0.000001	- 0.000001	-	-	- 0.000001	- 0.000001	-	-	- 0.000001	- 0.000001	-	-

$\theta_{el.0\_scaled}$	- 0.000001	0.000001	-	-	- 0.000001	0.000001	-	-	- 0.000001	0.000001	-	-
$\theta_{el.1\_scaled}$	-	- 0.000002	-	-	-	- 0.000002	-	-	-	- 0.000002	-	-
$\theta_{e\_FIX}$	-	-	0.03	-	-	-	0.17	-	-	-	0.27	-
$\theta_{in\_FIX}$	-	-	0.01	-	-	-	0.05	-	-	-	0.19	-
$\theta_{out\_FIX}$	-	-	- 0.04	-	-	-	- 0.19	-	-	-	- 0.3	-
$\theta_{e\_ALT}$	-	-	-	0.12	-	-	-	0.66	-	-	-	0.6
$\theta_{in\_ALT}$	-	-	-	0.07	-	-	-	0.31	-	-	-	0.48
$\theta_{out\_ALT}$	-	-	-	- 0.56	-	-	-	- 0.74	-	-	-	- 0.55

272 The results obtained from the PK/PD analysis using an individual modelling are shown in  
273 Figure 4, Figure 5, and Figure 6, while the results illustrated in Figure 7, Figure 8, and Figure  
274 9 present the PK/PD analysis using a population modelling. The parameter estimation and the  
275 simulation results obtained from the work, have been qualitatively verified by using the  
276 compartmental modelling approach. As can be seen from the following figures, the dynamic  
277 simulations agree closely with the parameter estimation results, and the model predictions are  
278 in good accordance with the clinical data. However, depending on the type of the objective  
279 function and the choice of individual modelling approach or population modelling approach,  
280 various results of the study highlighted several feasible configurations of the system. Such  
281 considerations were taken into account to aid decision making for further research. The  
282 values of the objective function obtained for each case study are reported in Table 7 and  
283 Table 8, which give an indication of the solution accuracy. According to the results, the  
284 objective function values observed for the PD parameter estimation are much higher than  
285 those obtained for the PK parameter estimation. This is because of the extensive PD data set  
286 and the widespread existence of fluctuations in the PD clinical data. Another potential  
287 contributor is the existence of hypothetical effect compartment that acts as a link between the  
288 PK and PD models. However, the analysis shows that a good match is obtained between the  
289 clinical data and the model predictions. The pharmacokinetic analysis in this work  
290 demonstrates how the overall performance of the PK parameter estimation problem depends  
291 on the optimisation algorithms and the objective functions. Making such comparisons  
292 between an absolute objective function and a scaled objective function lead to the fact that  
293 using a scaling factor may cause an algorithm to determine a different optimal solution. The  
294 absolute and scaled objective function values vary with no observable trend. Hence, based on  
295 a trade-off between the objective function values and the simulation results, a decision is  
296 made to use a set of parameters for subsequent computational studies.

297

**Patient 4**

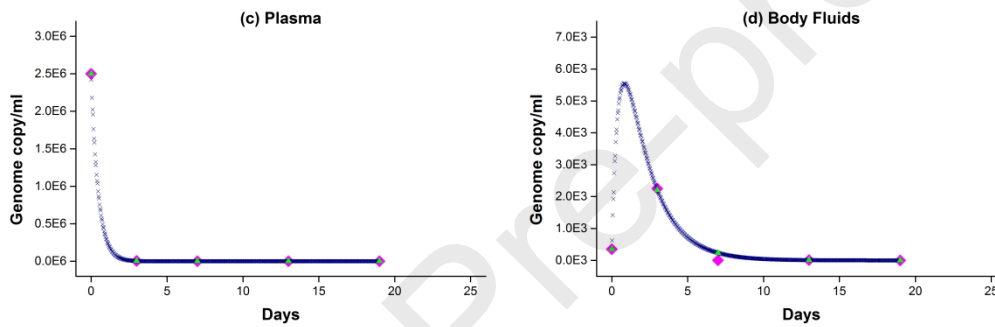


298

299

300

**Patient 6**

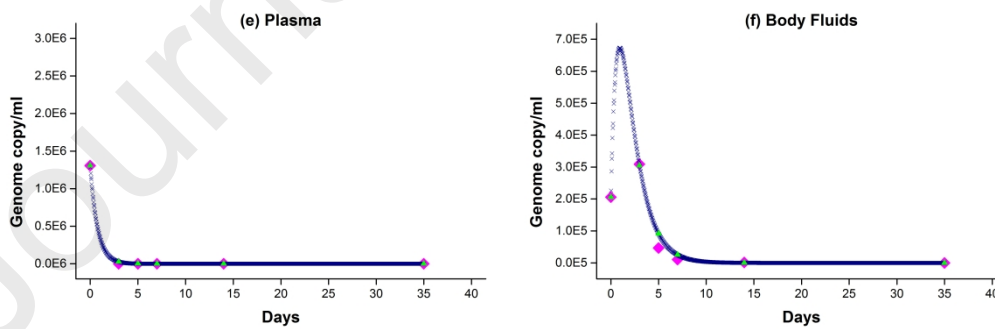


301

302

303

**Patient 9**



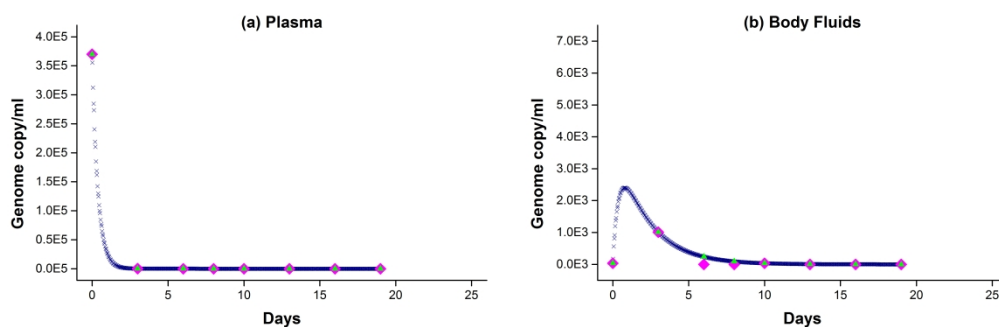
- ◆ Clinical data
- ▲ Parameter estimation using analytical solution
- × Model simulation for estimated parameters using OCFE

304

305 **Figure 4:** Pharmacokinetic Analysis, individually for each patient – Comparison of the PK model predictions  
 306 (using an absolute objective function) with the clinical data.

307

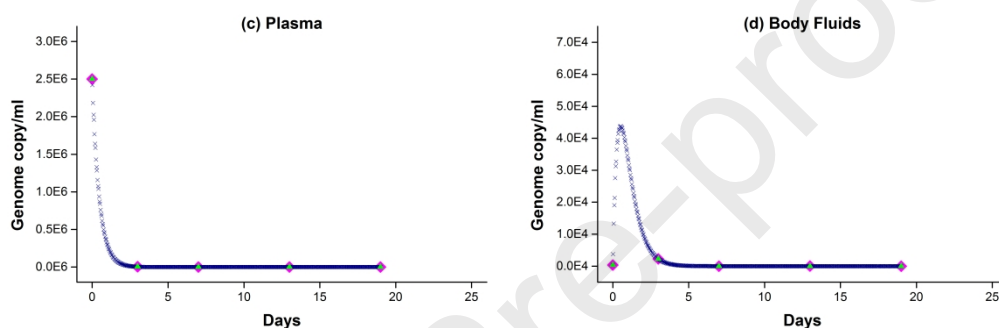
**Patient 4**



308

309

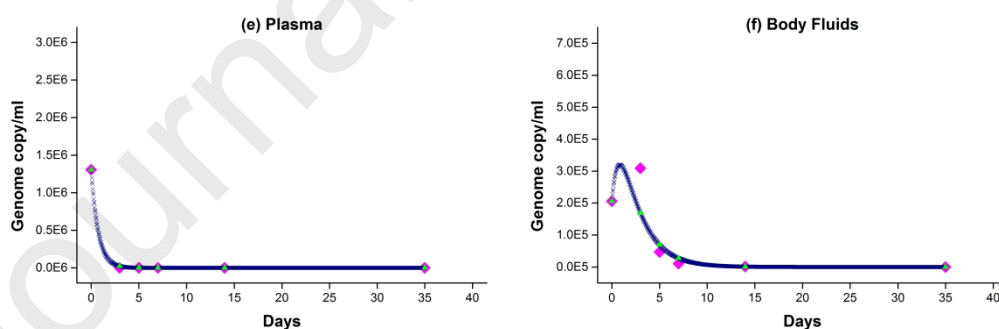
310

**Patient 6**

311

312

313

**Patient 9**

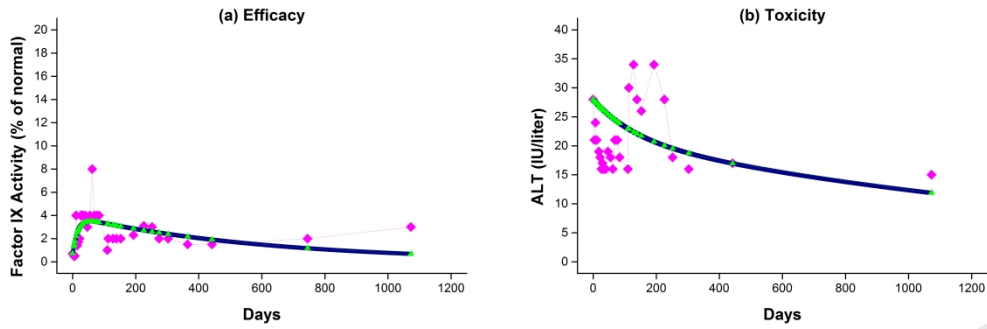
- ◆ Clinical data
- ▲ Parameter estimation using analytical solution
- × Model simulation for estimated parameters using OCFE

314

315 **Figure 5:** Pharmacokinetic Analysis, individually for each patient – Comparison of the PK model predictions  
 316 (using a scaled objective function) with the clinical data.

317

**Patient 4**

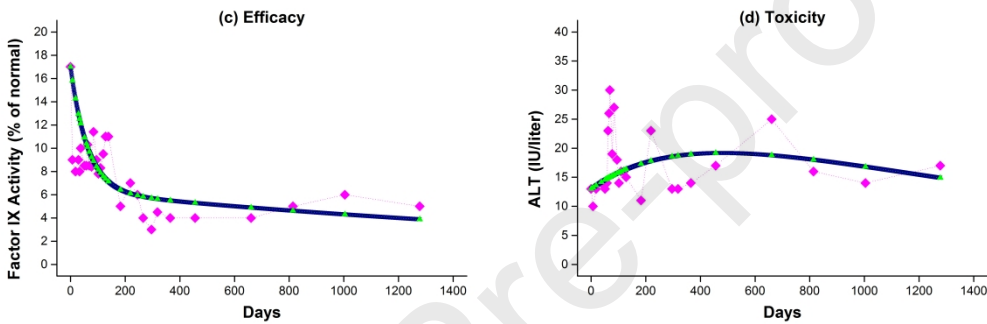


318

319

320

**Patient 6**

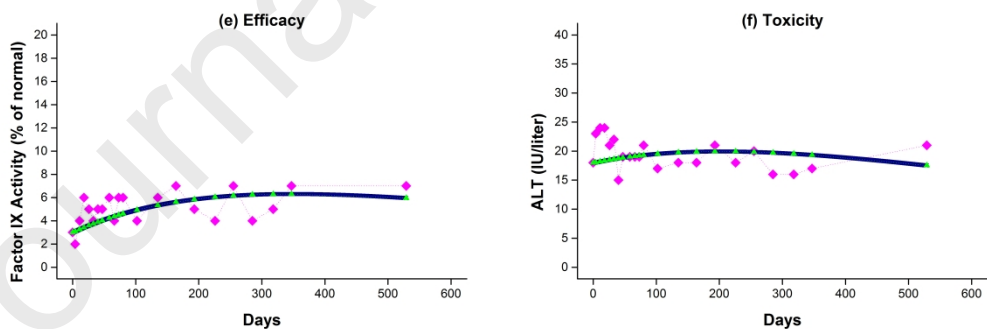


321

322

323

**Patient 9**



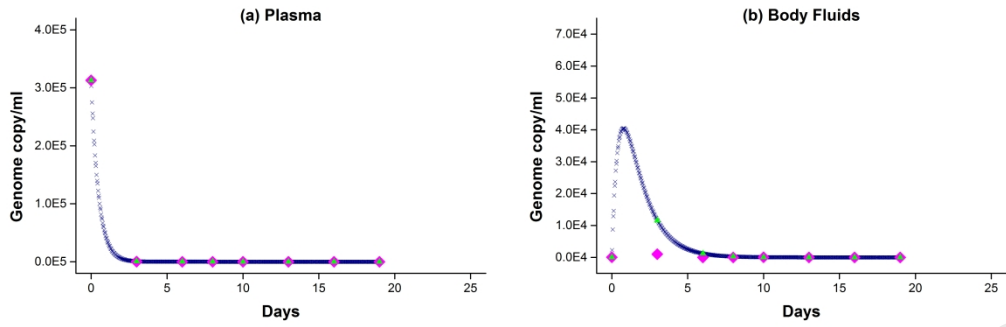
◆ Clinical data  
 ▲ Parameter estimation using analytical solution  
 × Model simulation for estimated parameters using OCFE

324

325 **Figure 6:** Pharmacodynamic Analysis, individually for each patient – Comparison of the PD model predictions  
 326 (using an absolute objective function) with the clinical data.

327

**Patient 4**

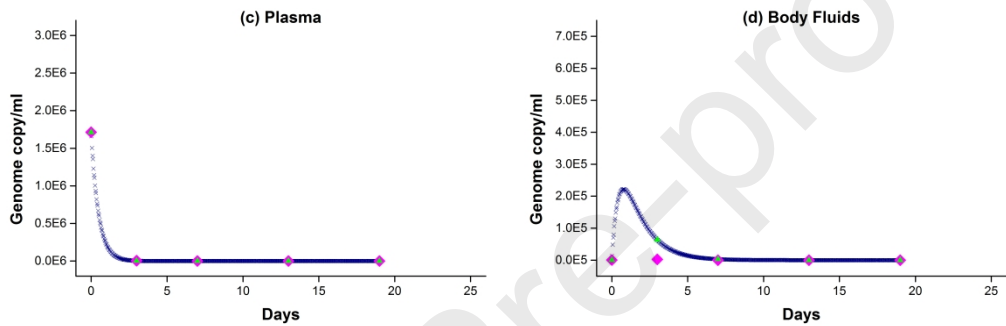


328

329

330

**Patient 6**

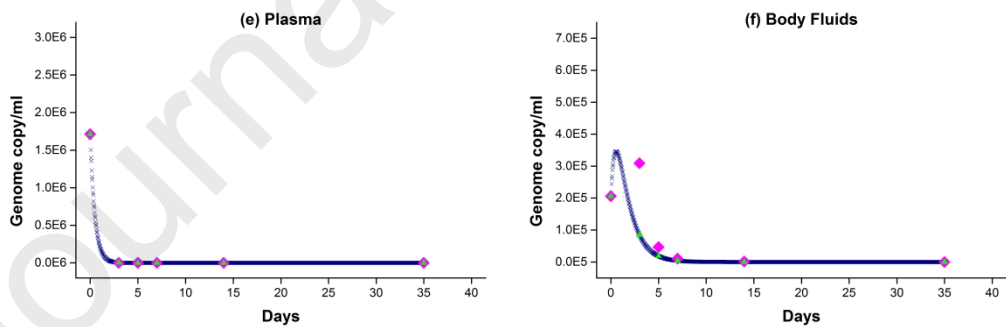


331

332

333

**Patient 9**



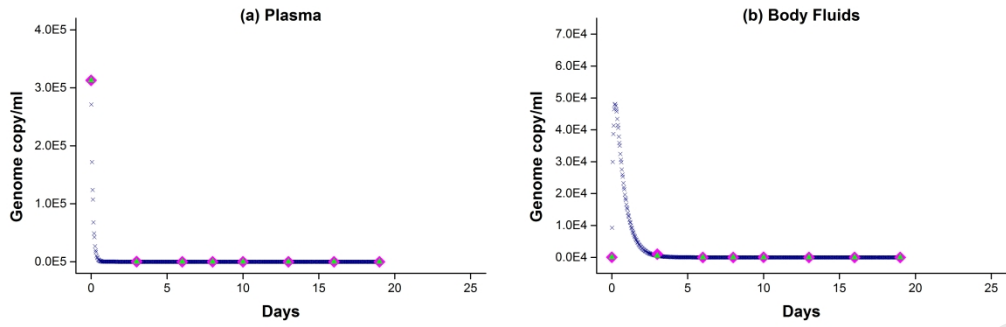
◆ Clinical data  
 ▲ Parameter estimation using analytical solution  
 × Model simulation for estimated parameters using OCFE

334

335 **Figure 7:** Pharmacokinetic Analysis, for all patients simultaneously – Comparison of the PK model predictions  
 336 (using an absolute objective function) with the clinical data.

337

**Patient 4**

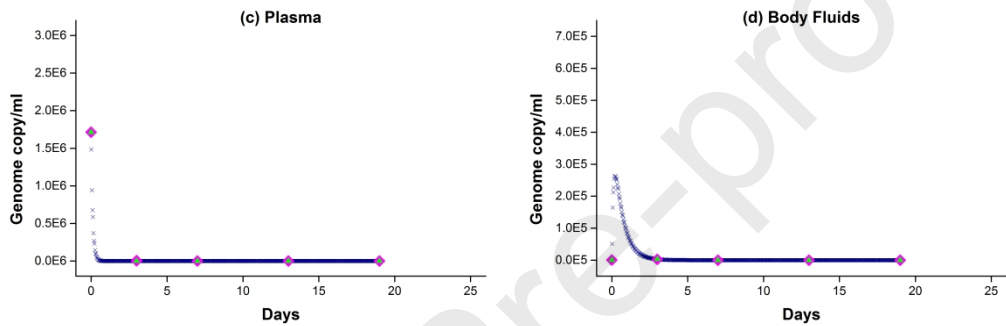


338

339

340

**Patient 6**

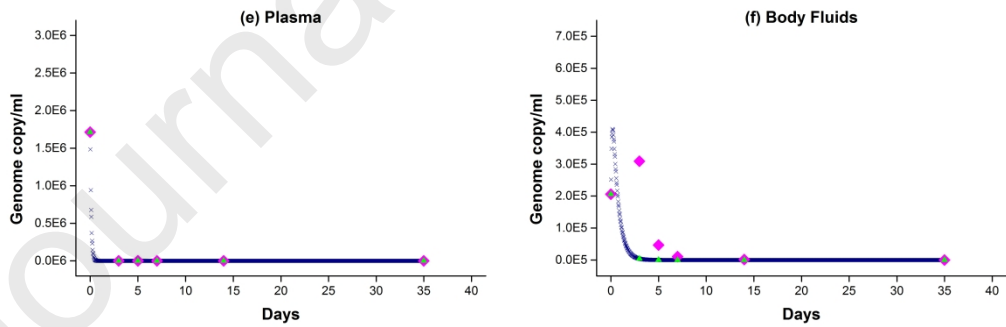


341

342

343

**Patient 9**



- ◆ Clinical data
- ▲ Parameter estimation using analytical solution
- × Model simulation for estimated parameters using OCFE

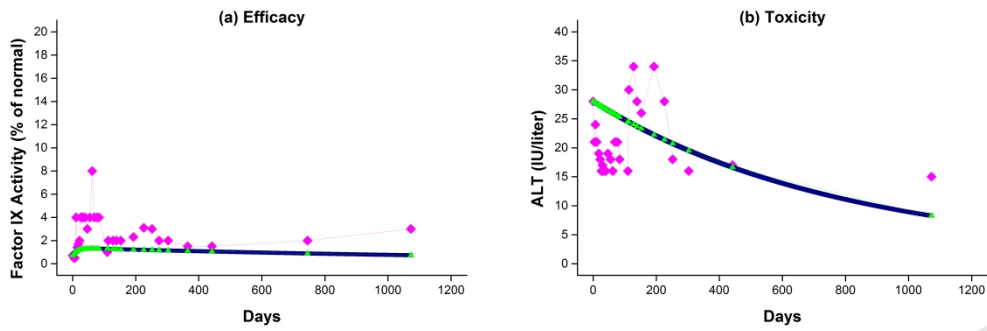
344

345 **Figure 8:** Pharmacokinetic Analysis, for all patients simultaneously – Comparison of the PK model predictions  
 346 (using a scaled objective function) with the clinical data.

347

**Patient 4**



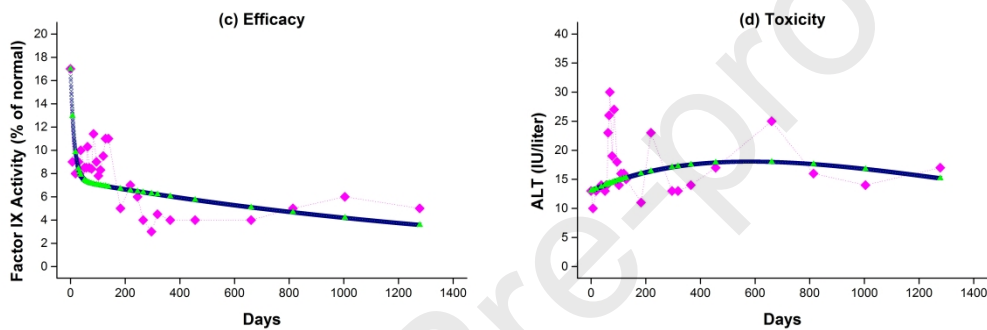


348

349

350

**Patient 6**

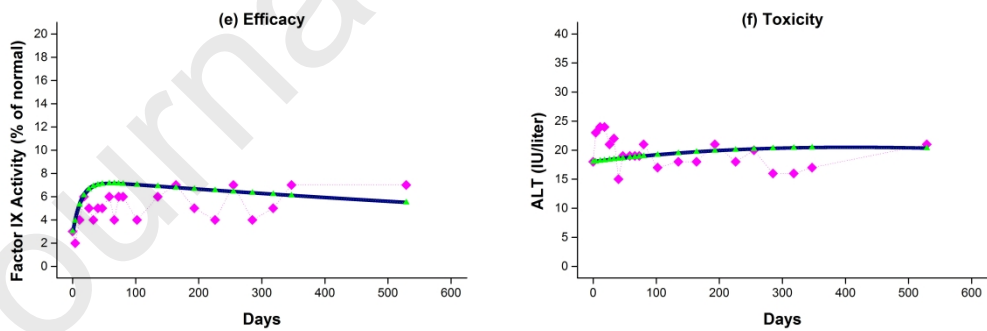


351

352

353

**Patient 9**



- ◆ Clinical data
- Parameter estimation using analytical solution
- Model simulation for estimated parameters using OCFE

354

355 **Figure 9:** Pharmacodynamic Analysis, for all patients simultaneously – Comparison of the PD model  
 356 predictions (using an absolute objective function) with the clinical data.

357 **Table 7:** Computational results for the individual modelling approach.

<b>Patient 4</b>		
	Objective function values	Corresponding figures
<b>PK Model</b>	$\text{Err}_{\text{absolute}} = 1.2013 \times 10^{-5}$	Figure 4 (a) and (b)
	$\text{Err}_{\text{scaled}} = 1.667 \times 10^{-16}$	Figure 5 (a) and (b)
<b>PD Model - FIX</b>	$\text{Err}_{\text{absolute}} = 52.140$	Figure 6 (a)
<b>PD Model - ALT</b>	$\text{Err}_{\text{absolute}} = 1399.890$	Figure 6 (b)

358

<b>Patient 6</b>		
	Objective function values	Corresponding figures
<b>PK Model</b>	$\text{Err}_{\text{absolute}} = 1.0396 \times 10^{-5}$	Figure 4 (c) and (d)
	$\text{Err}_{\text{scaled}} = 2.990$	Figure 5 (c) and (d)
<b>PD Model - FIX</b>	$\text{Err}_{\text{absolute}} = 200.021$	Figure 6 (c)
<b>PD Model - ALT</b>	$\text{Err}_{\text{absolute}} = 799.967$	Figure 6 (d)

359

<b>Patient 9</b>		
	Objective function values	Corresponding figures
<b>PK Model</b>	$\text{Err}_{\text{absolute}} = 3 \times 10^{-1}$	Figure 4 (e) and (f)
	$\text{Err}_{\text{scaled}} = 2.997$	Figure 5 (e) and (f)

<b>PD Model - FIX</b>	$\text{Err}_{\text{absolute}} = 37.134$	Figure 6 (e)
<b>PD Model - ALT</b>	$\text{Err}_{\text{absolute}} = 187.068$	Figure 6 (f)

360

361 **Table 8:** Computational results for the population modelling approach.

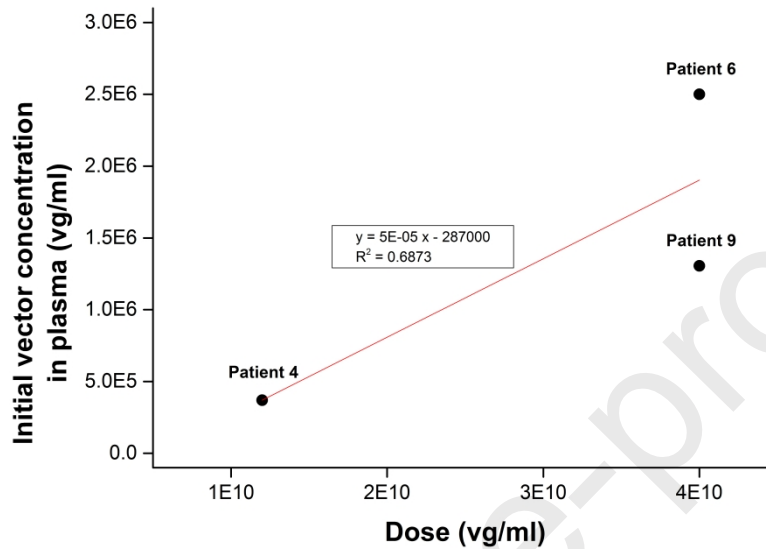
<b>Patients 4, 6, and 9</b>		
	Objective function values	Corresponding figures
<b>PK Model</b>	$\text{Err}_{\text{absolute}} = 1481.198$	Figure 7
	$\text{Err}_{\text{scaled}} = 10.270$	Figure 8
<b>PD Model - FIX</b>	$\text{Err}_{\text{absolute}} = 1011.102$	Figure 9 (a), (c), and (e)
<b>PD Model - ALT</b>	$\text{Err}_{\text{absolute}} = 4167.984$	Figure 9 (b), (d), and (f)

362

363

### 364 3.3 Initial Dose Selection

365 This section aims to explore how the simulation-based modelling approach can assist in the  
 366 initial dose selection. In this work, the initial doses used for the simulations are calculated  
 367 based on the following assumptions: (i) the average plasma volume is 50 ml/kg (Yiengst and  
 368 Shock, 1962); and (ii) there is a linear relationship between the dose administered (after  
 369 conversion from vg/kg to vg/ml) and the initial vector concentration in plasma.

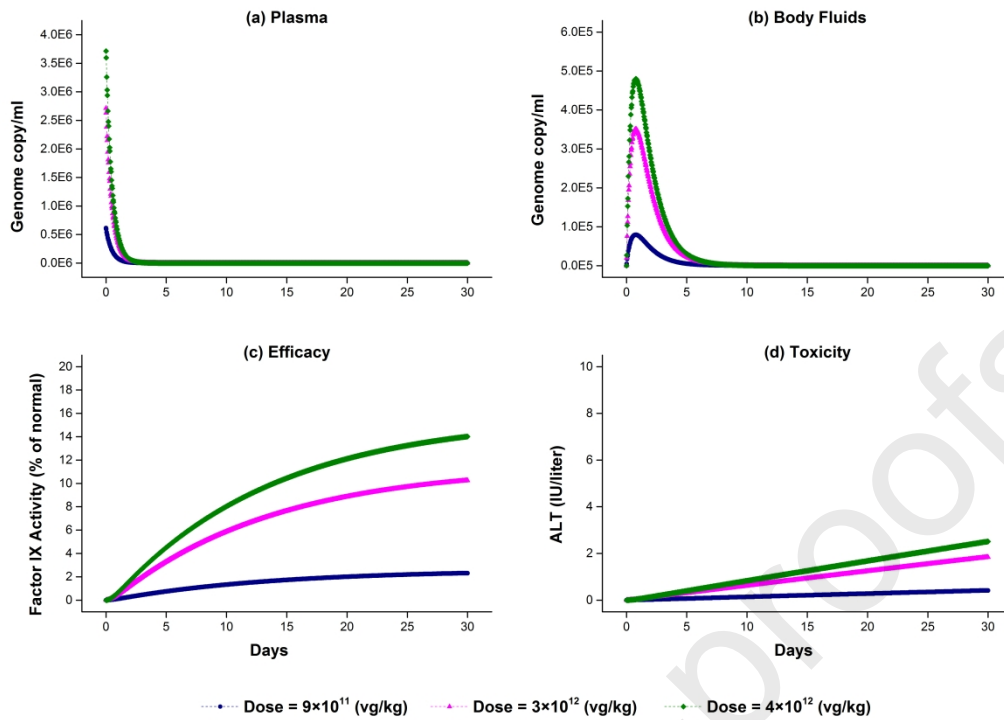


370

371 **Figure 10:** Linear regression curve between the dose administered and the initial vector concentration in  
 372 plasma.

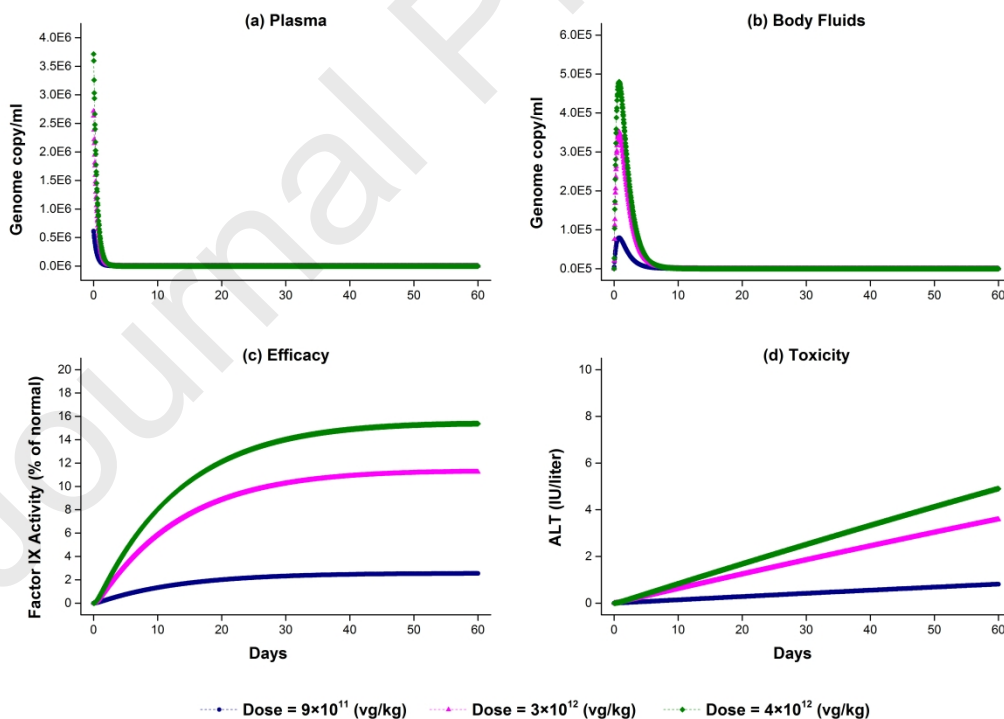
373 Linear regression is one of the most commonly used techniques to investigate the relationship  
 374 between two quantitative variables (Bewick et al., 2003). Therefore, a linear regression  
 375 analysis was carried out to determine the equation of the regression line, which is as follows  
 376 and shown in Figure 10: Initial vector concentration in plasma =  $5 \times 10^{-5} \times \text{Dose} - 287000$   
 377 .

378 For comparison purposes, the dynamic simulations were carried out for different time periods  
 379 and for various initial bolus doses. The PK/PD profiles are shown in Figure 11, Figure 12,  
 380 Figure 13, and Figure 14.



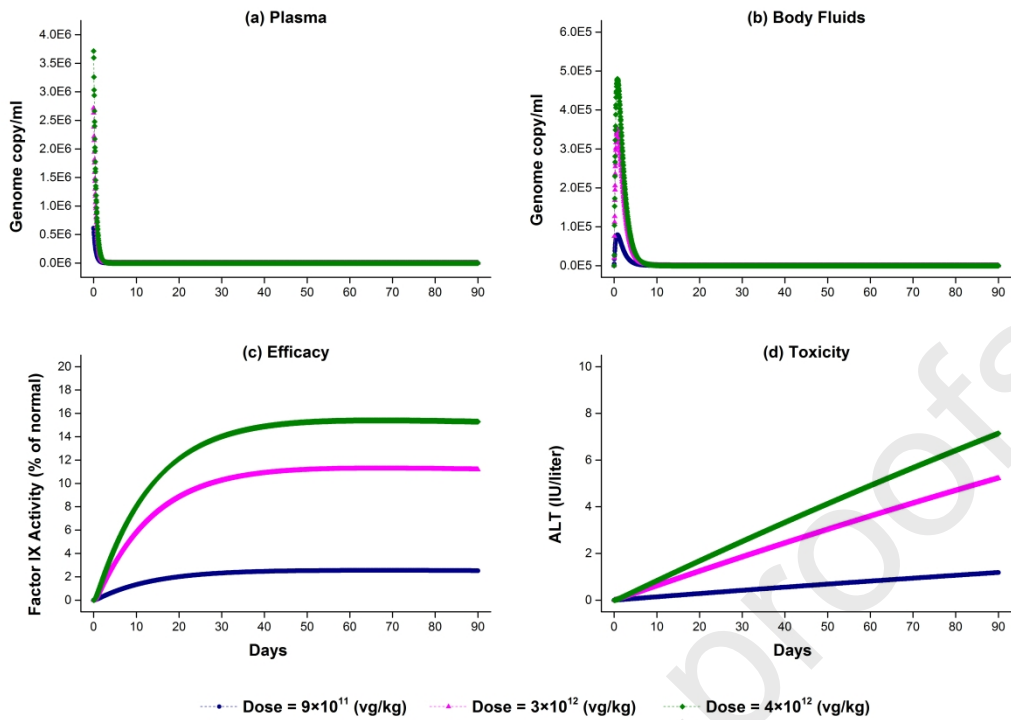
381

382 **Figure 11:** Population pharmacokinetic and pharmacodynamic results over a period of 30 days for different  
 383 initial bolus doses.



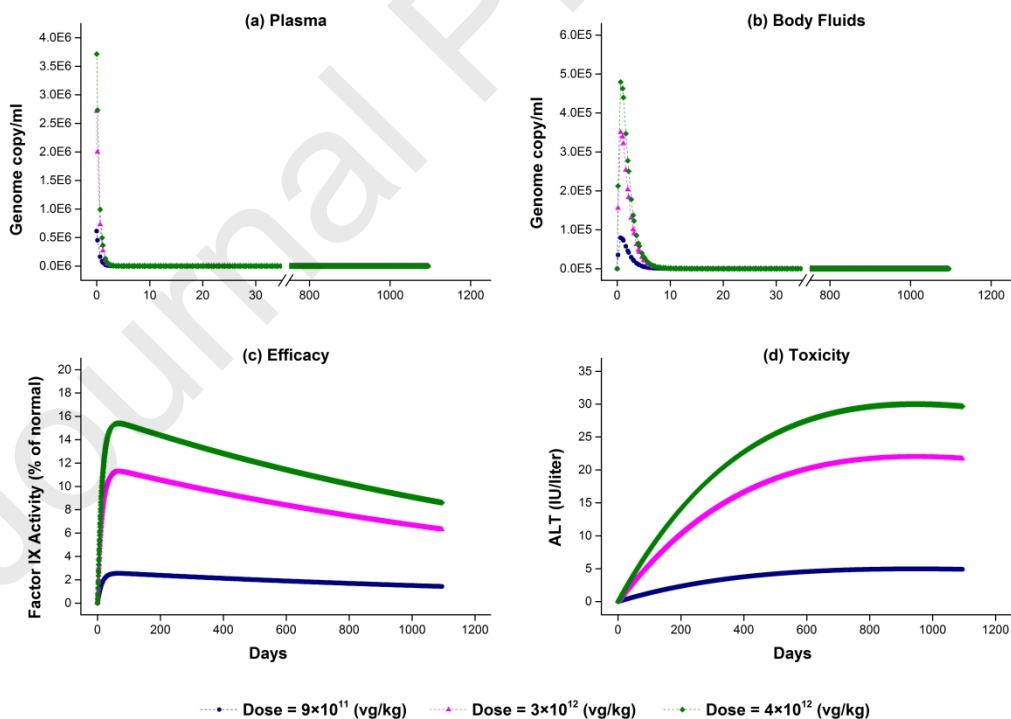
384

385 **Figure 12:** Population pharmacokinetic and pharmacodynamic results over a period of 60 days for different  
 386 initial bolus doses.



387

388 **Figure 13:** Population pharmacokinetic and pharmacodynamic results over a period of 90 days for different  
 389 initial bolus doses.



390

391 **Figure 14:** Population pharmacokinetic and pharmacodynamic results over a period of 3 years for different  
 392 initial bolus doses.

393 As can be seen in Figure 11b, Figure 12b, Figure 13b, and Figure 14b, the vector is expected  
394 to be eliminated from the body within 10 days after administration. The simulation results  
395 (Figure 11, Figure 12, Figure 13, and Figure 14) demonstrated that the increase in both factor  
396 IX activity and ALT level is dose-dependent, which is one of the key findings that is  
397 consistent with the work by Nathwani et al. (2014). In a recent study by Nathwani and  
398 Tuddenham (2020), the authors reported that the highest level of transgene expression of  
399 between 8% and 12% of normal was observed in the patients treated at the dose level of  $2 \times$   
400  $10^{12}$  vg/kg, which remained stable up to six weeks after gene transfer. The simulation results  
401 in this paper (Figure 12c, Figure 13c, and Figure 14c) lead to similar conclusion where FIX  
402 activity levels between 11% and 15% of normal can be observed for the high-dose subjects  
403 (dose level of  $3 \times 10^{12}$  vg/kg and  $4 \times 10^{12}$  vg/kg), which remained stable within three  
404 months after infusion. However, the ALT levels are increased consistently, especially in  
405 higher dose cohorts, which subsequently leads to a relative reduction in factor IX levels  
406 (about 55% reduction). According to Nathwani et al. (2014), the increase in the ALT level is  
407 associated with a decline in factor IX activity levels, suggesting a loss of transduced  
408 hepatocytes. Despite the drop in the level of expression, the simulation analysis found  
409 evidence for long-term efficacy as the FIX expression levels are maintained in the 6-10%  
410 range in the high-dose patients within a period of three years (Figure 14c), suggesting a  
411 reduction in FIX concentrate usage. This is in line with the findings reported by Nathwani  
412 and Tuddenham (2020), demonstrating that the transgenic FIX activity levels have remained  
413 stable over a period of 10 years follow-up and reduced the need for treatments with FIX  
414 concentrates.

#### 415 **4 Conclusions**

416 In this paper, a mathematical modelling approach was developed for gene transfer of adeno-  
417 associated viral vectors in patients with haemophilia B. The model-based platform discussed  
418 in this paper incorporates the pharmacokinetics and pharmacodynamics of the scAAV2/8-  
419 LP1-hFIXco vectors. The PK/PD model parameters were estimated using the analytical  
420 solution of the model, individually for each patient in a dose-independent manner, and for all  
421 patients simultaneously in a dose-dependent manner. A number of dynamic simulations were  
422 also carried out using OCFE for the validation of the model, demonstrating the simulation  
423 results are comparable to that obtained from parameter estimation. The simulation-based  
424 PK/PD modelling approach was then used for the initial dose selection to provide clinicians  
425 with better tools to make the decision-making process simpler for designing more effective  
426 treatment plans, which can be tailored to maximise efficacy while minimising toxicity for  
427 individual patients.

428 The authors have no conflict of interest to declare.

429

430 **5 References**

- 431 Banks, G. A., Roselli, R. J., Chen, R. & Giorgio, T. D. (2003) A model for the analysis of  
432 nonviral gene therapy. *Gene Therapy*, 10(20), 1766-1775.
- 433 Berraondo, P., Gonzalez-Aseguinolaza, G. & Troconiz, I. F. (2009) Semi-mechanistic  
434 pharmacodynamic modelling of gene expression and silencing processes. *European Journal*  
435 *of Pharmaceutical Sciences*, 37(3-4), 418-426.
- 436 Bewick, V., Cheek, L. & Ball, J. (2003) Statistics review 7: correlation and regression.  
437 *Critical Care*, 7(6), 451-459.
- 438 Degasperi, A., Fey, D. & Kholodenko, B. N. (2017) Performance of objective functions and  
439 optimisation procedures for parameter estimation in system biology models. *NPJ Systems*  
440 *Biology and Applications*, 3(1), 20.
- 441 Dinh, A. T., Pangarkar, C., Theofanous, T. & Mitragotri, S. (2007) Understanding  
442 intracellular transport processes pertinent to synthetic gene delivery via stochastic simulations  
443 and sensitivity analyses. *Biophysical Journal*, 92(3), 831-846.
- 444 Franchini, M., Frattini, F., Crestani, S. & Bonfanti, C. (2012) Haemophilia B: current  
445 pharmacotherapy and future directions. *Expert Opinion on Pharmacotherapy*, 13(14), 2053-  
446 2063.
- 447 Gabrielsson, J. & Weiner, D. (2010) Pharmacokinetic and pharmacodynamic data analysis:  
448 concepts and applications, 4th ed. Sweden: Swedish Pharmaceutical Press.
- 449 George, L. A., Sullivan, S. K., Giermasz, A., Rasko, J. E. J., Samelson-Jones, B. J., Ducore,  
450 J. et al. (2017) Hemophilia B gene therapy with a high-specific-activity factor IX variant.  
451 *New England Journal of Medicine*, 377(23), 2215-2227.
- 452 Holz, M. & Fahr, A. (2001) Compartment modeling. *Advanced Drug Delivery Reviews*,  
453 48(2-3), 249-264.
- 454 Horobin, R. W. & Weissig, V. (2005) A QSAR-modeling perspective on cationic transfection  
455 lipids. 1. predicting efficiency and understanding mechanisms. *Journal of Gene Medicine*,  
456 7(8), 1023-1034.
- 457 Howard, E. L., Becker, K. C. D., Rusconi, C. P. & Becker, R. C. (2007) Factor IXa inhibitors  
458 as novel anticoagulants. *Arteriosclerosis Thrombosis and Vascular Biology*, 27(4), 722-727.
- 459 Jamili, E. & Dua, V. (2018) Optimal model-based control of non-viral siRNA delivery.  
460 *Biotechnology and Bioengineering*, 115(7), 1866-1877.
- 461 Jandt, U., Shao, S., Wirth, M. & Zeng, A. P. (2011) Spatiotemporal modeling and analysis of  
462 transient gene delivery. *Biotechnology and Bioengineering*, 108(9), 2205- 2217.
- 463 Ledley, T. S. & Ledley, F. D. (1994) Multicompartment, numerical-model of cellular events  
464 in the pharmacokinetics of gene therapies. *Human Gene Therapy*, 5(6), 679- 691.
- 465 Manno, C. S., Arruda, V. R., Pierce, G. F., Glader, B., Ragni, M., Rasko, J. et al. (2006)  
466 Successful transduction of liver in hemophilia by AAV-Factor IX and limitations imposed by



- 467 the host immune response. *Nature Medicine*, 12(3), 342-347.
- 468 Martin, T. M., Wysocki, B. J., Wysocki, T. A. & Pannier, A. K. (2015) Identifying  
469 intracellular pDNA losses from a model of nonviral gene delivery. *IEEE Transactions on*  
470 *Nanobioscience*, 14(4), 455-464.
- 471 Nathwani, A. C., Davidoff, A., Hanawa, H., Zhou, J. F., Vanin, E. F. & Nienhuis, A. W.  
472 (2001) Factors influencing in vivo transduction by recombinant adeno-associated viral  
473 vectors expressing the human factor IX cDNA. *Blood*, 97(5), 1258-1265.
- 474 Nathwani, A. C., Davidoff, A. M. & Tuddenham, E. G. D. (2017) Gene Therapy for  
475 Hemophilia. *Hematology-Oncology Clinics of North America*, 31(5), 853-868.
- 476 Nathwani, A. C., Gray, J. T., McIntosh, J., Ng, C. Y. C., Zhou, J. F., Spence, Y. et al. (2007)  
477 Safe and efficient transduction of the liver after peripheral vein infusion of self-  
478 complementary AAV vector results in stable therapeutic expression of human FIX in  
479 nonhuman primates. *Blood*, 109(4), 1414-1421.
- 480 Nathwani, A. C., Gray, J. T., Ng, C. Y. C., Zhou, J. F., Spence, Y., Waddington, S. N. et al.  
481 (2006) Self-complementary adeno-associated virus vectors containing a novel liver-specific  
482 human factor IX expression cassette enable highly efficient transduction of murine and  
483 nonhuman primate liver. *Blood*, 107(7), 2653-2661.
- 484 Nathwani, A. C., Reiss, U. M., Tuddenham, E. G. D., Rosales, C., Chowdary, P., McIntosh,  
485 J. et al. (2014) Long-term safety and efficacy of factor IX gene therapy in hemophilia B. *New*  
486 *England Journal of Medicine*, 371(21), 1994-2004.
- 487 Nathwani, A. C., Rosales, C., McIntosh, J., Rastegarlar, G., Nathwani, D., Raj, D. et al.  
488 (2011a) Long-term safety and efficacy following systemic administration of a self-  
489 complementary AAV vector encoding human FIX pseudotyped with serotype 5 and 8 capsid  
490 proteins. *Molecular Therapy*, 19(5), 876-885.
- 491 Nathwani, A. C., Tuddenham, E. G. D., Rangarajan, S., Rosales, C., McIntosh, J., Linch, D.  
492 C. et al. (2011b) Adenovirus-associated virus vector-mediated gene transfer in hemophilia B.  
493 *New England Journal of Medicine*, 365(25), 2357-2365.
- 494 Nathwani, A. C., Tuddenham, E. G. D. (2020) Haemophilia, the journey in search of a cure.  
495 1960-2020. *British Journal of Haematology*, 191(4), 573-578.
- 496 Nestorov, I. (2003) Whole body pharmacokinetic models. *Clinical Pharmacokinetics*, 42(10),  
497 883-908.
- 498 Patel, N., Reiss, U., Davidoff, A. M. & Nathwani, A. C. (2014) Progress towards gene  
499 therapy for haemophilia B. *International Journal of Hematology*, 99(4), 372-376.
- 500 Powell, J. S., Pasi, K. J., Ragni, M. V., Ozelo, M. C., Valentino, L. A., Mahlangu, J. N. et al.  
501 (2013) Phase 3 study of recombinant factor IX Fc fusion protein in hemophilia B. *New*  
502 *England Journal of Medicine*, 369(24), 2313-2323.
- 503 Ramaswamy, S., Tonnu, N., Tachikawa, K., Limphong, P., Vega, J. B., Karmali, P. P.,  
504 Chivukula, P. & Verma, I. M. (2017) Systemic delivery of factor IX messenger RNA for  
505 protein replacement therapy. *Proceedings of the National Academy of Sciences of the United*

- 506 States of America, 114(10), E1941-E1950.
- 507 Tsang, T. C., Bentley, D. R., Mibashan, R. S. & Giannelli, F. (1988) A factor-IX mutation,  
508 verified by direct genomic sequencing, causes haemophilia-B by a novel mechanism. *EMBO*  
509 *Journal*, 7(10), 3009-3015.
- 510 Varga, C. M., Hong, K. & Lauffenburger, D. A. (2001) Quantitative analysis of synthetic  
511 gene delivery vector design properties. *Molecular Therapy*, 4(5), 438-446.
- 512 Varga, C. M., Tedford, N. C., Thomas, M., Klibanov, A. M., Griffith, L. G. & Lauffenburger,  
513 D. A. (2005) Quantitative comparison of polyethylenimine formulations and adenoviral  
514 vectors in terms of intracellular gene delivery processes. *Gene Therapy*, 12(13), 1023-1032.
- 515 Washington, I. M. & Van Hoosier, G. (2012) Clinical biochemistry and hematology. In:  
516 Suckow, M. A., Stevens, K. A. & Wilson, R. P. (eds), *The Laboratory Rabbit, Guinea Pig,*  
517 *Hamster, and Other Rodents. American College of Laboratory Animal Medicine Series. San*  
518 *Diego: Elsevier Academic Press Inc, 57-116.*
- 519 Yiengst, M. J. & Shock, N. W. (1962) Blood and plasma volume in adult males. *Journal of*  
520 *Applied Physiology*, 17(2), 195.

521 **Declaration of interests**

522

523  The authors declare that they have no known competing financial interests or personal  
524 relationships that could have appeared to influence the work reported in this paper.

525

526  The authors declare the following financial interests/personal relationships which may be  
527 considered as potential competing interests:

528

529

530

531

532

533

534

535 **Declaration of interests**

536

537  The authors declare that they have no known competing financial interests or personal  
538 relationships that could have appeared to influence the work reported in this paper.

539

540  The authors declare the following financial interests/personal relationships which may be  
541 considered as potential competing interests:

542

543

544

545

546

547

548

549

550

551

552

553

554

- A promising platform for gene delivery clinical trial simulations is provided
- PK/PD analysis is performed for both individual and population modelling approaches
- Model predictions are consistent with the clinical data for haemophilia patients
- A simulation-based modelling approach is proposed to guide initial dose selection
- Simulations show that the increase in FIX activity and ALT level is dose-dependent

Journal Pre-proofs